



ELSEVIER

Available online at [www.sciencedirect.com](http://www.sciencedirect.com)

SCIENCE @ DIRECT®

Nuclear Instruments and Methods in Physics Research A 507 (2003) 445–449

**NUCLEAR  
INSTRUMENTS  
& METHODS  
IN PHYSICS  
RESEARCH**  
Section A[www.elsevier.com/locate/nima](http://www.elsevier.com/locate/nima)

# Measurements of nonlinear harmonic radiation and harmonic microbunching in a visible SASE FEL

A. Tremaine<sup>a,\*</sup>, X.J. Wang<sup>b</sup>, M. Babzien<sup>b</sup>, I. Ben-Zvi<sup>b</sup>, M. Cornacchia<sup>c</sup>,  
R. Malone<sup>b</sup>, A. Murokh<sup>d</sup>, H.-D. Nuhn<sup>c</sup>, C. Pellegrini<sup>d</sup>, S. Reiche<sup>d</sup>,  
J. Rosenzweig<sup>d</sup>, J. Skaritka<sup>b</sup>, V. Yakimenko<sup>b</sup>

<sup>a</sup>Lawrence Livermore National Laboratory, Livermore, CA 94550, USA

<sup>b</sup>Brookhaven National Laboratory, Upton, NY 11973, USA

<sup>c</sup>Stanford Linear Accelerator Center, Stanford, CA 94309, USA

<sup>d</sup>University of California, Los Angeles, Los Angeles, CA 90095, USA

---

## Abstract

The experimental characterization of nonlinear harmonic generation (NHG) and electron beam microbunching at saturation from a visible SASE FEL are presented in this report. The gain lengths, spectra and energies of NHG were experimentally measured up to the third harmonic, and agree with theoretical predictions. Electron beam microbunching in both the fundamental and the second harmonic as the function of the SASE output were experimentally observed over the full range of SASE gain. The bunching factors for both the fundamental ( $b_1$ ) and second harmonic ( $b_2$ ) were experimentally characterized at saturation. The microbunching data provides another test of SASE saturation as well as correlating the NHG and electron beam microbunching modes to the fundamental SASE. © 2003 Published by Elsevier Science B.V.

PACS: 41.60.Cr; 41.60.Ap; 4185.Ja

Keywords: Nonlinear; Harmonic; Saturation; Microbunching

---

## 1. Introduction

The motivation to obtain very short wavelength, high brightness light sources has increased the interest in X-ray FELs. These SASE (single pass) FELs are designed to produce hard X-rays with peak brilliances [1,2] that are several orders of magnitude larger than current light sources. A consequence from high fundamental gain in FELs

is the production of nonlinear harmonic radiation (NHR) [3–5]. NHR can have significant power and offers shorter wavelengths over the fundamental radiation, thus extending the applications of these future X-ray FEL facilities.

This report details the NHR and electron beam microbunching measurements in a visible SASE FEL. The second and third NHR have high power and sharp spectra, making them another source of quality radiation. Second NHR is unique to low energy, planar undulator FELs like VISA, but the studies presented here of the third NHR can be

---

\*Corresponding author.

E-mail address: [tremaine@llnl.gov](mailto:tremaine@llnl.gov) (A. Tremaine).

directly applied to future X-ray FELs; the LCLS [1], for example could expect high power, narrow bandwidth 5 Å NHR. The longitudinal microbunching of the electron beam, integral the SASE process, drives not only the fundamental radiation, but also the NHR. The present measurements correlate NHR to the fundamental radiation through the electron beam microbunching structure at high FEL gain.

## 2. Experimental design

The experimental results presented here were performed using the Visible to Infrared SASE Amplifier (VISA) FEL at Brookhaven's Accelerator Test Facility. An S-band photocathode RF gun operating in the longitudinal emittance compensation mode [6] produces a high brightness electron beam that is accelerated to an energy of 70 MeV by two SLAC type linac sections [7]. A quadrupole triplet provides the final matching of the electron beam into the undulator. The novel undulator is 4 m long, has a 1.8 cm period with built-in strong focusing quadrupoles. The combination of the high brightness electron beam and unique undulator significantly enhance the FEL performance (shorten the gain length), which is crucial to reducing the size of this [8] and other single pass devices. Table 1 shows the VISA FEL design parameters, and another publication [9] details the measured electron beam dynamics.

Eight diagnostic pop-in ports are spaced along the 4-m undulator with an additional diagnostic station 30 cm downstream of the undulator.

Energy vs. distance measurements for the three lowest SASE modes were made along the second half of the undulator. The electron beam microbunching was measured in the post undulator diagnostic station using CTR [10,11]. Employing a unique foil and mirror set-up [12], simultaneous capture of both the microbunching and SASE energy per FEL micropulse was possible.

## 3. Experimental results

NHR and harmonic microbunching in an FEL occur just before and at peak performance of the fundamental mode. Fig. 1 shows data of the evolution of the nonlinear harmonic spectra for different FEL gain.

Another publication [5] compares the spectra of these nonlinear modes to the fundamental at saturation. At low gain the radiation for both nonlinear modes is just developing, and the spectra broad. As nonlinear gain increases, spectral narrowing continues until a sharp peak at each mode is reached. The VISA SASE FEL couples strongly to the second and third NHR, where the spectra sharpen with increasing harmonic number,  $n$ ; the FWHM for the fundamental [5], second and

Table 1  
VISA FEL design parameters

Wavelength (fundamental) $\lambda$	800 nm
E-beam energy, $E$	72 MeV
Peak current, $I$	200 A
Emittance, $\epsilon$	2 mm-mrad
Power gain length, $L$	17.5 cm
Spot size, $\sigma$	60 $\mu\text{m}$

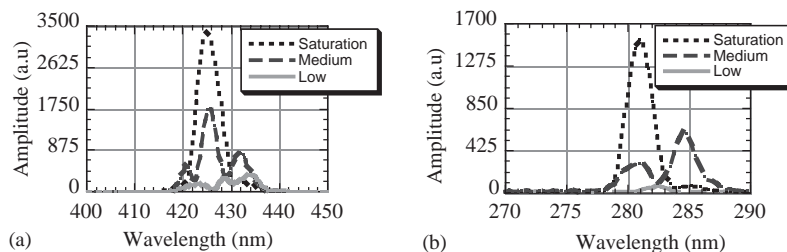


Fig. 1. NHR SASE FEL spectra at various FEL gain for the second (a) and third (b) modes. The spectrometer resolution is about 1 nm.

third NHR are 15, 6 and 3 nm, respectively. The third NHR spectra at large SASE gain demonstrates that high quality NHR can be obtained in SASE FELs, a result applicable to future short wavelength devices.

Compared to the harmonic radiation produced in FELs [3,4], NHR has shorter gain lengths and higher energies. The signature of the NHR gain length,  $L_{gn}$ , is  $L_{g,n} = L_{g,1}/n$ , where  $L_{g,1}$  is the fundamental SASE gain length. Fig. 2 [5] shows the energy vs. distance data on a semi-log plot along the length of the undulator for the three lowest modes. The fundamental radiation deviates from the exponential, an indication of SASE saturation. For the second and third harmonic modes, the transition into the nonlinear regime is clearly established at 3.25 and 3.75 m, respectively, and the gain lengths confirm nonlinear harmonic theory:  $L_{g,1} = 19.0$  cm,  $L_{g,2} = 9.8$  cm and  $L_{g,3} = 6.0$  cm.

Table 2 compares the energy for the three FEL modes at the end of the undulator. An analytical relationship between the energies of the second,  $E_2$ , and third,  $E_3$ , modes is given by [4],

$$E_2 \approx E_3 \left( \frac{K}{\gamma k_u \sigma_x} \right)^2 \left( \frac{K_2}{K_3} \right)^2 \left( \frac{b_2}{b_3} \right)^2 \quad (1)$$

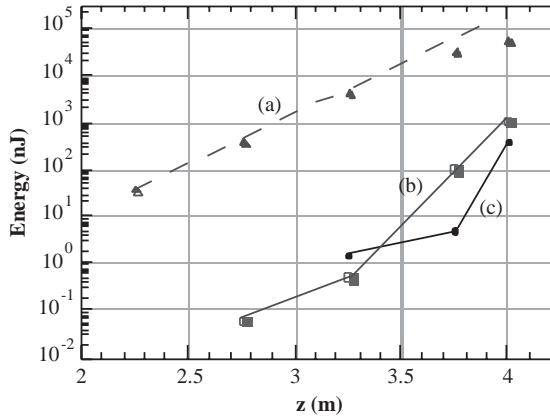


Fig. 2. Measured Energy vs. distance for the fundamental (a), second (b) and third (c) nonlinear harmonics along the second half of the 4-m undulator. The transfer from the linear from nonlinear regime is seen at 3.25 and 3.75 m for the second and third harmonics, respectively. The gain lengths are 19, 9.8 and 6.0 cm, respectively.

Table 2

Measured harmonic energy for fundamental, second and third harmonics

Mode (n)	Wavelength (nm)	Energy ( $\mu$ J)	% of fundamental energy
1	845	52	—
2	425	0.93	1.8
3	280	0.4	0.77

where  $K_n$  are the coupling coefficients,  $\gamma$  is the electron beam energy,  $k_u$  is the undulator wave number,  $K$  is the undulator parameter,  $b_n$  are the bunching parameters and  $\sigma_x$  is the transverse spot size. Coupling to the even harmonic is enhanced in low  $\gamma$ , planar undulator FELs because of the inverse relationship between mode energy and electron beam energy. The design of the VISA FEL causes the second harmonic energy to exceed the third,  $E_2 = 1.6E_3$ , giving a unique window to further test nonlinear harmonic theory. The third NHR has about 1% of the fundamental as expected and coupled to the sharp spectra measured in Fig. 1, this FEL produces about 1 MW of spectrally narrow UV radiation for an 85  $\mu$ m pulse length [9]. Extending these results to future X-ray FELs, the LCLS, for example, could obtain 0.1 GW of third NHR.

Microbunching in the electron beam drives both the SASE and NHR. To estimate the microbunching factors, a CTR foil assembly was used. The total CTR energy is given by [11]

$$U_n = \frac{N^2 e^2 b_n^2}{8\sqrt{\pi} \sigma_x \sigma_y \sigma_z} \left( \frac{\gamma}{nk_r} \right)^4 \left( \frac{1}{\sigma_x^2} + \frac{1}{\sigma_y^2} \right) \quad (2)$$

where  $N$  is the number of electrons in the bunch,  $\sigma_{x,y,z}$  are the transverse ( $x, y$ ) and longitudinal ( $z$ ) beams sizes, respectively,  $k_r$  is the fundamental wave number of the microbunching,  $n$  is the harmonic number, and  $b_n$  is the microbunching factor for the  $n$ th harmonic. By measuring the amount of CTR energy emitted, Eq. (2) can be used to estimate the depth of the SASE induced electron beam modulation. Fig. 3 compares the optical transition radiation (OTR) emitted to the CTR, which contains the microbunching information, when the electron beam strikes an aluminium

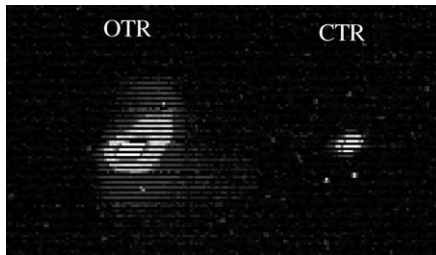


Fig. 3. OTR and CTR for the VISA electron beam after exiting the undulator.

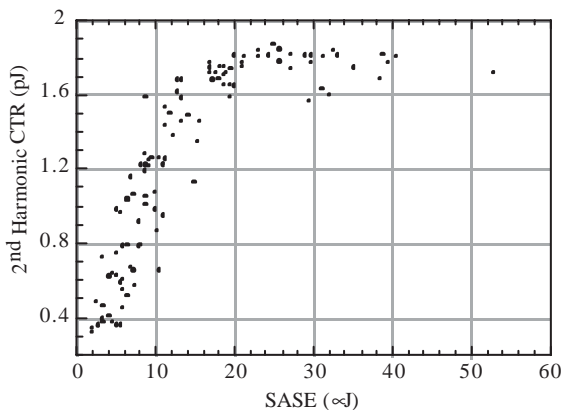


Fig. 4. Measured second harmonic CTR vs. SASE. Beam is longitudinally microbunched at a period of 425 nm.

foil. As expected, the CTR is emitted in a much narrower cone than the OTR and to capture just the CTR, two bandpass filters, giving an attenuation of  $10^6$  outside the bandpass, were placed in front of the detector.

Fig. 4 [12] shows the second harmonic CTR vs. SASE for each micropulse over the full range of FEL gain. Similar to the fundamental microbunching, the second nonlinear harmonic microbunching stops growing at the time when the fundamental radiation approaches saturation (see Fig. 2). The FEL gain process depends on the electrons becoming more densely packed over the radiation wavelength, and as the FEL goes into saturation an oscillator exchange of energy occurs between the electron beam and radiation field. Using Eq. (2), the peak fundamental microbunching (at 845 nm) factor measured at the monitor was  $b_1 = 0.50$  (data not shown). Simulations using GENESIS [13], which include the post undulator

drift to the foil, predict a bunching factor of  $b_1 = 0.52$ , which agrees closely to the measurement. Fig. 4 shows the data for the second nonlinear harmonic microbunching (at 425 nm) vs. SASE where a bunching factor at the diagnostic station of  $b_2 = 0.13$  is obtained from the data and Eq. (2). GENESIS simulations predict  $b_2 = 0.2$ .

Because the fundamental SASE mode drives the higher harmonics, the second microbunching mode depends more strongly on the SASE than does the fundamental microbunching. The second harmonic microbunching is in less agreement with prediction than the fundamental. The discrepancy between predicted and measured second harmonic microbunching may be due to a variety of factors, such as the uncertainty in the de-bunching, to which higher harmonics are more sensitive. Also, the assumption of a Gaussian electron beam longitudinal distribution may also have contributed since the bunch shape may display some non-Gaussian structure [9].

#### 4. Conclusion

These results are a comprehensive verification of the nonlinear harmonic generation process in SASE FELs. The three lowest modes of radiation were characterized and compare nicely to nonlinear theory with a slight discrepancy for the second harmonic microbunching. The driving mechanism of radiation in FELs is the microbunching. The fundamental and harmonic microbunching were characterized and at saturation, the FEL shows strong microbunching with periods of 845 and 425 nm. The correlation between the NHR, microbunching and fundamental SASE mode has been experimentally established.

#### References

- [1] M. Cornacchia, et al., Linac coherent light source (LCLS) design study report, Report SLAC-R-521, SLAC, CA, revised 1998.
- [2] R. Brinkmann, G. Materlik, J. Rossbach, A. Wagner (Eds.), Conceptual design of a 500 GeV  $e^+ e^-$  linear collider with integrated X-ray laser facility, DESY Report

- DESY97-048, Deutsches Elektronen-Synchrotron, Hamburg, 1997.
- [3] R. Bonifacio, et al., Nucl. Instr. and Meth. A 293 (1990) 627.
  - [4] Z. Huang, K.J. Kim, Phys. Rev. E 62 (2000) 7295.
  - [5] A. Tremaine, et al., Phys. Rev. Lett. 88 (2002) 204801.
  - [6] X.J. Wang, et al., Phys. Rev. E 62 (2002) 7295.
  - [7] X.J. Wang, et al., Proceedings of 1999 Particle Accelerator Conference, New York, Vol. 3459, 1999.
  - [8] P. Emma, et al., in: Proceedings of the 20th International FEL Conference (FEL'98), Williamsburg, VA, USA, 1198, SLAC-PB-7913.
  - [9] A. Murokh, et al., Phys. Rev. E (2003), in press.
  - [10] J. Rosenzweig, G. Travish, A. Tremaine, Nucl. Instr. and Meth. A 365 (1995) 255.
  - [11] A. Tremaine, et al., Phys. Rev. Lett. 81 (1998) 5816.
  - [12] A. Tremaine, et al., Phys. Rev. E 66 (2002) 036503.
  - [13] S. Reiche, Nucl. Instr. and Meth. A 429 (1999) 243.